



Separating Direct and Indirect Turbofan Engine Combustion Noise While Estimating Post-Combustion (Post-Flame) Residence Time Using the Correlation Function

Jeffrey Hilton Miles
Glenn Research Center, Cleveland, Ohio

NASA STI Program . . . in Profile

Since its founding, NASA has been dedicated to the advancement of aeronautics and space science. The NASA Scientific and Technical Information (STI) program plays a key part in helping NASA maintain this important role.

The NASA STI Program operates under the auspices of the Agency Chief Information Officer. It collects, organizes, provides for archiving, and disseminates NASA's STI. The NASA STI program provides access to the NASA Aeronautics and Space Database and its public interface, the NASA Technical Reports Server, thus providing one of the largest collections of aeronautical and space science STI in the world. Results are published in both non-NASA channels and by NASA in the NASA STI Report Series, which includes the following report types:

- **TECHNICAL PUBLICATION.** Reports of completed research or a major significant phase of research that present the results of NASA programs and include extensive data or theoretical analysis. Includes compilations of significant scientific and technical data and information deemed to be of continuing reference value. NASA counterpart of peer-reviewed formal professional papers but has less stringent limitations on manuscript length and extent of graphic presentations.
- **TECHNICAL MEMORANDUM.** Scientific and technical findings that are preliminary or of specialized interest, e.g., quick release reports, working papers, and bibliographies that contain minimal annotation. Does not contain extensive analysis.
- **CONTRACTOR REPORT.** Scientific and technical findings by NASA-sponsored contractors and grantees.

- **CONFERENCE PUBLICATION.** Collected papers from scientific and technical conferences, symposia, seminars, or other meetings sponsored or cosponsored by NASA.
- **SPECIAL PUBLICATION.** Scientific, technical, or historical information from NASA programs, projects, and missions, often concerned with subjects having substantial public interest.
- **TECHNICAL TRANSLATION.** English-language translations of foreign scientific and technical material pertinent to NASA's mission.

Specialized services also include creating custom thesauri, building customized databases, organizing and publishing research results.

For more information about the NASA STI program, see the following:

- Access the NASA STI program home page at <http://www.sti.nasa.gov>
- E-mail your question via the Internet to help@sti.nasa.gov
- Fax your question to the NASA STI Help Desk at 443-757-5803
- Telephone the NASA STI Help Desk at 443-757-5802
- Write to:
NASA Center for AeroSpace Information (CASI)
7115 Standard Drive
Hanover, MD 21076-1320



Separating Direct and Indirect Turbofan Engine Combustion Noise While Estimating Post-Combustion (Post-Flame) Residence Time Using the Correlation Function

Jeffrey Hilton Miles
Glenn Research Center, Cleveland, Ohio

Prepared for the
48th Aerospace Sciences Meeting
sponsored by the American Institute of Aeronautics and Astronautics
Orlando, Florida, January 4–7, 2010

National Aeronautics and
Space Administration

Glenn Research Center
Cleveland, Ohio 44135

Trade names and trademarks are used in this report for identification only. Their usage does not constitute an official endorsement, either expressed or implied, by the National Aeronautics and Space Administration.

This work was sponsored by the Fundamental Aeronautics Program at the NASA Glenn Research Center.

Level of Review: This material has been technically reviewed by technical management.

Available from

NASA Center for Aerospace Information
7115 Standard Drive
Hanover, MD 21076-1320

National Technical Information Service
5301 Shawnee Road
Alexandria, VA 22312

Available electronically at <http://www.sti.nasa.gov>

Separating Direct and Indirect Turbofan Engine Combustion Noise While Estimating Post-Combustion (Post-Flame) Residence Time Using the Correlation Function

Jeffrey Hilton Miles
National Aeronautics and Space Administration
Glenn Research Center
Cleveland, Ohio 44135

Summary

A previous investigation on the presence of direct and indirect combustion noise for a full-scale turbofan engine using a far-field microphone at 130° is extended by also examining signals obtained at two additional downstream directions using far-field microphones at 110° and 160°. A generalized cross-correlation function technique is used to study the change in propagation time to the far field of the combined direct and indirect combustion noise signal as a sequence of low-pass filters are applied. The filtering procedure used produces no phase distortion. As the low-pass filter frequency is decreased, the travel time increases because the relative amount of direct combustion noise is reduced. The indirect combustion noise signal travels more slowly because in the combustor entropy fluctuations move with the flow velocity, which is slow compared to the local speed of sound. The indirect combustion noise signal travels at acoustic velocities after reaching the turbine and being converted into an acoustic signal. The direct combustion noise is always propagating at acoustic velocities. The results show that the estimated indirect combustion noise time delay values (post-combustion residence times) measured at each angle are fairly consistent with one another for a relevant range of operating conditions and demonstrate source separation of a mixture of direct and indirect combustion noise. The results may lead to a better idea about the acoustics in the combustor and may help develop and validate improved reduced-order physics-based methods for predicting turbofan engine core noise.

Introduction

Combustion noise can make a significant contribution to overall turbofan engine noise at low-power settings, which are typical of approach flight. In addition, technological advancement in aircraft engine-cycle design and noise-reduction methods may reduce jet and fan noise even at higher engine power settings, where they currently are of more importance than combustion noise. With the pending development of reduced gaseous emission aircraft engine combustors, the gaps in combustor noise source knowledge have increased in importance. Consequently, the prediction and measurement of combustion noise is an area of increased interest. The low-frequency contribution of combustion noise, both direct and indirect, is a unique characteristic feature of combustion noise and differentiates it from fan and jet noise. Combustion noise is difficult to study because hydrodynamic and acoustic pressure fluctuations are intermixed at the source location. Taking measurements at the source location is also challenging because of the combustor environment. In addition, much of the far-field noise is not correlated with the combustor and/or turbine internal noise. However, the part that is correlated can be studied using signal cross-correlation functions and coherence functions. Studying this part can improve our understanding of the acoustics in combustors and may ultimately enable development of improved reduced-order physics-based methods for predicting direct and indirect combustor noise.

Cross-correlation functions were used by Miles (Refs. 1 and 2) with low-pass filters to investigate direct and indirect combustion noise source separation based on signal propagation time delays. In the first paper by Miles (Ref. 1) only a single 30.5-m (100-ft) far-field microphone at 130° was used where

angles are measured from the upstream direction. The second paper by Miles (Ref. 2) extended the results using microphones at 110° and 160°.

The measurements at 130° discussed by Miles (Ref. 1) showed that using the cross-correlation function, time delays were identified in all cases, clearly indicating the combustor is the source of the noise. The low-frequency noise is a blend of indirect combustion noise, which is loudest for this engine in the 0- to 200-Hz frequency range, and direct combustion noise, which is loudest in the 200- to 400-Hz frequency range. Consequently, far-field microphone signals at 130°—both unfiltered and low-pass filtered at 400 Hz—had a cross-correlation time delay near 90 ms, while those low-pass filtered at less than 400 Hz had a cross-correlation time delay longer than 90 ms. Low-pass filtering at frequencies less than 400 Hz partially removes mainly the direct combustion noise signals. The remainder includes the indirect combustion noise signal, which travels more slowly because the propagation speed depends upon the entropy convection velocity in the combustor. Source separation of direct and indirect combustion noise was demonstrated by proper use of low-pass filters with the cross-correlation function for the same range of operating conditions used herein: namely, 48, 54, 60, and 71 percent of maximum power. The first investigation used a combustor pressure sensor and a far-field microphone at 130° to study the change in the indirect combustion noise time delay (the post-combustion residence time) with the low-pass filter frequency and operating condition. In the present report (an updated version of Ref. 2), in addition to the study being extended by including far-field microphones at 110° and 160° attention is directed to the fact that the estimated indirect combustion noise time delay can also be viewed as the post-combustion (post-flame) residence time of the entropy and combustion products in the cooled combustor section as they move with the flow velocity to the turbine entrance. This residence time is an ensemble average over all fuel nozzles in the combustor.

This cross-correlation function procedure is applied to data from a dual-spool TECH977 turbofan engine. Acoustic data from the same TECH977 engine test program are discussed by Miles (Refs. 3 and 4), Mendoza et al. (Ref. 5), Weir and Mendoza (Ref. 6), Schuster (Ref. 7), Royalty and Schuster (Ref. 8), Dougherty and Mendoza (Ref. 9), Weir (Ref. 10), and Hultgren and Miles (Ref. 11).

The research discussed herein is an extension of the study of the combustion noise of the TECH977 engine conducted by Miles (Refs. 3 and 4), using a cross-spectrum phase angle procedure and the cross-correlation function procedure used by Miles (Ref. 1). These reports indicate that for this particular engine, combustion noise occurs primarily in the 0- to 400-Hz frequency range. Miles (Ref. 1) also discusses previous relevant work in detail.

The fundamental premise of this report and References 1 and 2 is that filtering to remove frequencies above 400 Hz leaves the combined direct and indirect combustion noise unchanged in the signal. Filtering to remove frequencies above 200 Hz leaves the indirect combustion noise mostly unchanged. In addition, the low-pass filters are designed to eliminate phase angle modifications and to leave the signal delay time identified as the location of peak of the correlation function of random noise at the proper time value. Results are presented for an unfiltered condition, and after low-pass filtering to remove frequencies above 400, 300, 200, 150, and 100 Hz using a filtering procedure having no phase distortion. The idea of prefiltering the signals before doing a cross-correlation is discussed by Carter (Ref. 12) and Scarbrough et al. (Ref. 13), and the resulting function is identified as a generalized cross-correlation (GCC) function. However, any phase distortion produced by the filters used by Carter and Scarbrough et al. to create the GCC function they use does not appear to be a problem since it is not discussed in these papers. A special procedure is used herein to ensure no phase distortion is introduced.

An appendix listing the symbols used in this report is included to aid the reader.

Engine Noise Data and Analysis

The Honeywell TECH977 turbofan engine and the engine test data are discussed next. Then the generalized cross-correlation function technique is discussed.

Engine Test Data

The static engine test was conducted at Honeywell's San Tan outdoor acoustic test facility. A polar array of 32 ground-plane microphones was used. Each Brüel & Kjær 4134 microphone in an inverted stand with a 7-mm (0.3-in.) ground spacing was placed on a 30.5-m (100-ft) radius. The microphones were positioned from 5° to 160° (relative to the inlet) in 5° increments. The microphone array is shown in References 3, 5, 6, and 10.

The dual-spool, turbofan engine has a direct-drive, wide-chord fan connected by a long shaft to the low-pressure turbine spool and a high-pressure compressor connected by a concentric short shaft to the turbine high-pressure spool. The fan diameter is 86.9 cm (34.2 in.). The combustor design is a straight-through-flow annular geometry with 16 fuel nozzles and 2 igniters. One of the igniters is replaced by a pressure transducer, which is identified herein as CIP1. The dependent source separation technique used to identify direct and indirect combustion noise uses data from the CIP1 transducer and far-field microphones at 110° and 160°. Engine diagrams are shown (Refs. 3, 5, 6, 8, 9, and 10).

The data acquisition system had a sampling rate of 65 536 Hz and a sampling duration of roughly 70 s. This permitted data reduction using 254 overlapped ensemble averages at a bandwidth resolution of 2 Hz. Further signal estimation parameters are shown in Table I. Autospectra, coherent output power, aligned and unaligned coherence, aligned cross-spectra, as well as aligned and unaligned spectra are shown in Reference 3.

TABLE I.—SPECTRAL ESTIMATE PARAMETERS

Segment length, N , data points/segment	32 768
Sample rate, r_n , samples/s	65 536
Record length of segment, $\mathcal{T}_{ss} = N/r_n$, s	0.500
Sampling interval, $\Delta t = 1/r_n$, s	1/65 536
Bandwidth resolution, $B_e = \Delta f = 1/\mathcal{T}_{ss} = r_n/N$, Hz	2.0
Upper frequency limit, $f_u = 1/2\Delta t = r_n/2$, Hz	32 768
Number of frequencies, $n_f = f_u/\Delta f = N/2$	16 384
Propagation time delay ^a (lag), $D = 5927/65\,536$, ms	90.44
Number of independent samples, n_{ss}	128
Overlap	0.50
Total record length, \mathcal{T}_{tot} , s	≈ 70

^aAt temperature $\mathcal{T} = 9^\circ\text{C}$ (48 °F) and radial distance $r = 30.48$ m (100 ft), with microphone at 130°.

Correlation Functions

The autocorrelation function describes the general dependence of the values of function $x(t)$ at one time on the value the function $x(t + \theta)$ has at another time. It is the average product of the functions, $x(t)$ and $x(t + \theta)$ calculated over a time interval T , shifted relative to each by the time θ . The autocorrelation function is

$$R_{xx}(\theta) = \lim_{T \rightarrow \infty} \frac{1}{T} \int_0^T x(t)x(t + \theta)dt \quad (1)$$

The cross-correlation function describes the general dependence of the values of the function $x(t)$ at one time on the value of another function $y(t)$ at another time. It is the average product of the functions, $x(t)$ and $y(t + \theta)$ calculated over a time interval T , shifted relative to each other by the time θ .

The cross-correlation function is

$$R_{xy}(\theta) = R_{yx}(-\theta) = \lim_{T \rightarrow \infty} \frac{1}{T} \int_0^T x(t)y(t+\theta)dt \quad (2)$$

Note, the cross-correlation function is not symmetric in time about zero.

The normalized cross-correlation function known as the cross-correlation function coefficient (normalized cross-covariance function) used herein to plot the cross-correlation functions is defined as

$$\rho_{xy}(\theta) = \rho_{yx}(-\theta) = \frac{R_{xy}(\theta)}{\sqrt{R_{xx}(0)R_{yy}(0)}} \quad (3)$$

by Bendat and Piersol (Refs. 14 and 15). Although the total cross-correlation functions are calculated, only the positive time delay is shown in this report.

Figure 1 shows the normalized cross-correlation functions generated, using for $x(t)$ a random-number-generated white noise and for $y(t)$ the same random-number-generated white noise displaced by an amount $D = 86.98$ ms. Each plot in this figure has the cross-correlation function of the unfiltered signals and the signals filtered by the 100-Hz low-pass filter. In addition, Figures 1(a) to 1(d) have the results of the 400-, 300-, 200-, and 150-Hz low-pass filters, respectively. These plots show that the width of the peak increases as the filter design frequency is reduced. In each plot the peak is at 86.98 ms. In Reference 1, the normalized cross-correlation functions are a function of the time variable τ . In the present report, a distinction is made between the time variable used to calculate the cross-correlation function and the variable used to denote the time at which the cross-correlation function has a peak. Here, the normalized cross-correlation functions are a function of the time variable θ . The measured value of θ where the peak is located is a signal travel time (time delay value), and this value will be called a τ value. The set of θ values at which peaks occur in the normalized cross-correlation functions will be identified as being in the τ set of measured signal travel times. The normalized cross-correlation functions discussed herein are based on measurements at three angles ϕ and four power settings P , using no filter and five different filters. Consequently, the measured signal travel times analyzed are a set of values defined by $\tau(\phi, P, \eta)$. The angles used are $\phi = 110^\circ, 120^\circ$, and 160° . The power settings are at P percent maximum power where $P = 48, 54, 60$, and 71 percent. The effective low-pass filter frequencies are $\eta = 400, 300, 200, \approx 150$, and 100 Hz. The filter design is discussed in the next section.

Filtering

The 100-, 200-, 300-, and 400-Hz low-pass filters used are three-section Butterworth filters. The filters will be identified herein by the low-pass filter cutoff frequency, η . Filter design was done using bilinear transformation following a method described by Stearns and David (Ref. 16). These filter parameters are given in Tables 2, 4, 5, and 6 of the report by Miles (Ref. 1) on applying the procedure discussed herein to signals from the 130° far-field microphone.

To see if the results depended on the filter design approach, a three-section non-Butterworth filter was used as a 150-Hz low-pass filter with coefficients shown in Table 3 of Reference 1. For the first section, this filter uses the second-section filter values of the 300-Hz low-pass filter from Table 5 of Reference 1. For the second and third section, this filter uses the third-section filter values of the 300-Hz filter from Table 5 of Reference 1. The 150-Hz filter has a larger transition band than a properly designed Butterworth filter.

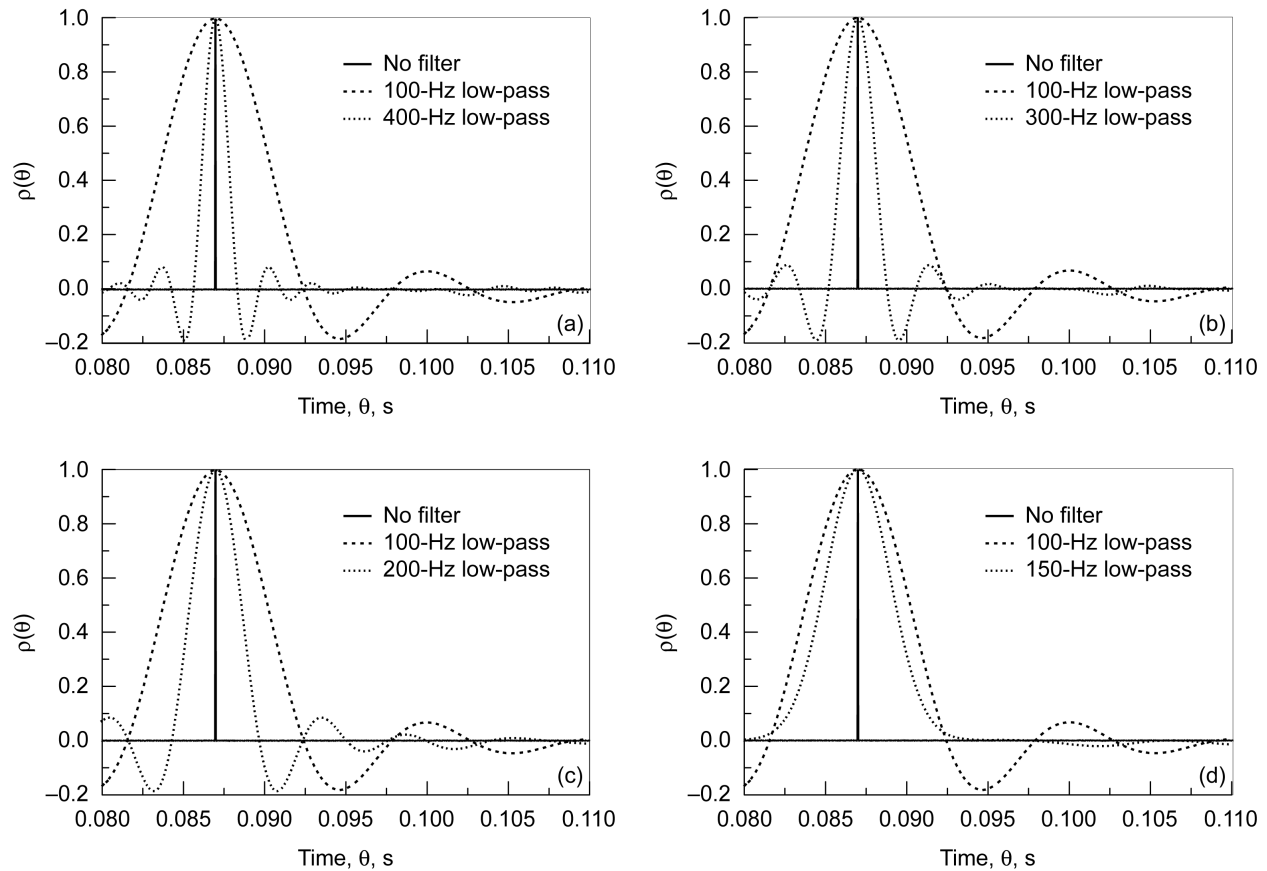


Figure 1.—Cross-correlation $\rho(\theta)$ with no filter and various low-pass filters of white noise displaced by $D_T = 5700/65\,536 = 86.9751$ ms. (a) 100- and 400-Hz low-pass filters. (b) 100- and 300-Hz low-pass filters. (c) 100- and 200-Hz low-pass filters. (d) 100- and 150-Hz low-pass filters.

To make certain the filters introduce no phase angle modification, the filter for each segment is applied to the forward time series and is then applied again, with the time reversed. The time series reversal is then removed before processing the next segment or quitting. This procedure is discussed by Kormylo and Jain (Ref. 17) and by Hamming (Ref. 18). Note the effective filter function is the square of the absolute value of the designed filter function.

In order to demonstrate the filtering process a study was conducted using white noise generated by use of a “Mersenne Twister” random number generator (Ref. 19). Figure 1 of Reference 1 shows the effect of each filter on the signal amplitude. This white noise generator was also used to create Figure 1 in this report.

Cross-Correlation With and Without Filtering

The sequence of low-pass filters, discussed in the previous section, is applied to the combustor pressure transducer signal and far-field microphone signal. The signal resulting from using the 400-Hz low-pass filter contains both indirect and direct combustion noise. By applying further low-pass filters in the sequence—300, 200, 150, and 100 Hz—the resulting signal will have a decreasing amount of direct combustion noise. The signal resulting from using the 100-Hz low-pass filter contains mainly indirect combustion noise.

The cross-correlation functions between the microphone at 110° and the combustor pressure sensor are presented in Figures 2 through 5, and the cross-correlation functions between the microphone at 160° and the combustor pressure sensor are presented in Figures 6 through 9. The figures show the cross-correlation functions in the time region, which contain the peak value. The left side of the peak is determined by the direct combustion noise, which moves at acoustic speeds along its full path. The right side of the peak in the region is controlled by the indirect combustion noise, which initially propagates with the mean flow velocity. The combustion noise spectrum has a limited frequency range. For this particular engine, this limit is about 400 Hz.

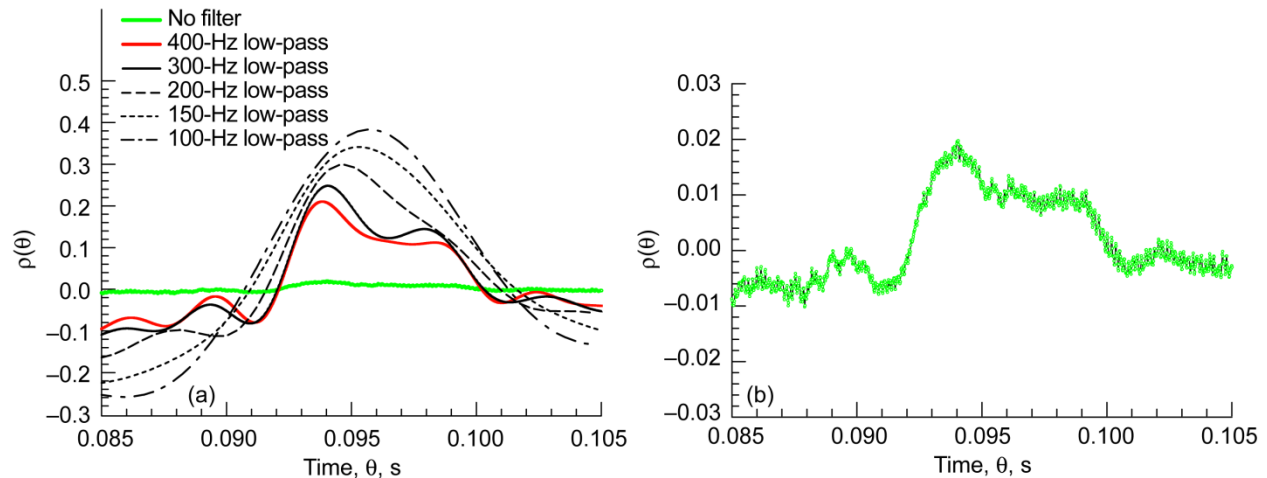


Figure 2.—Normalized cross-correlation, $\rho(\theta)$, using internal combustor pressure sensor and 110° far-field microphone, calculated using no filter and various low-pass filters at setting of 48 percent of maximum power in region of peak values. (a) 100- to 400-Hz low-pass filters. (b) No filter.

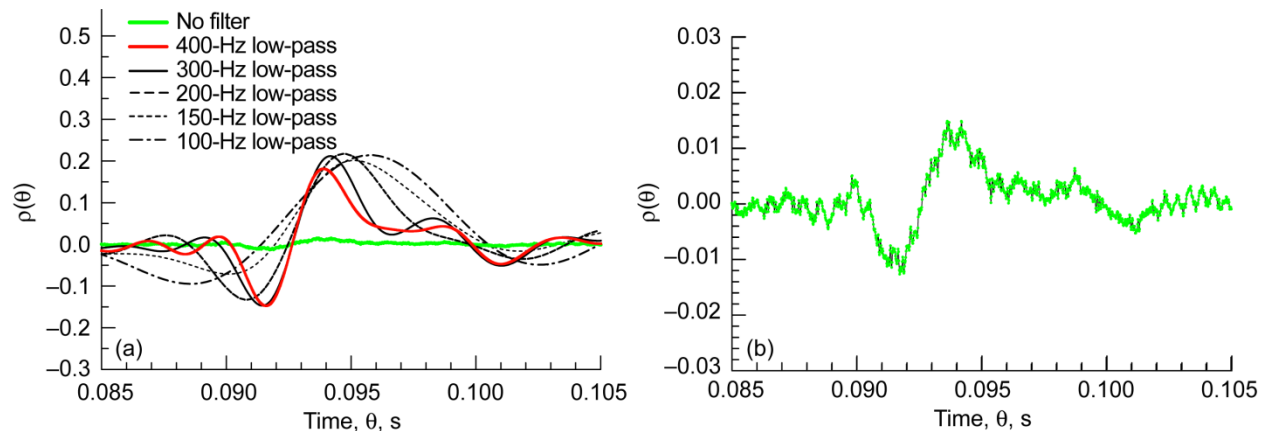


Figure 3.—Normalized cross-correlation, $\rho(\theta)$, using internal combustor pressure sensor and 110° far-field microphone, calculated using no filter and various low-pass filters at setting of 54 percent of maximum power in region of peak values. (a) 100- to 400-Hz low-pass filters. (b) No filter.

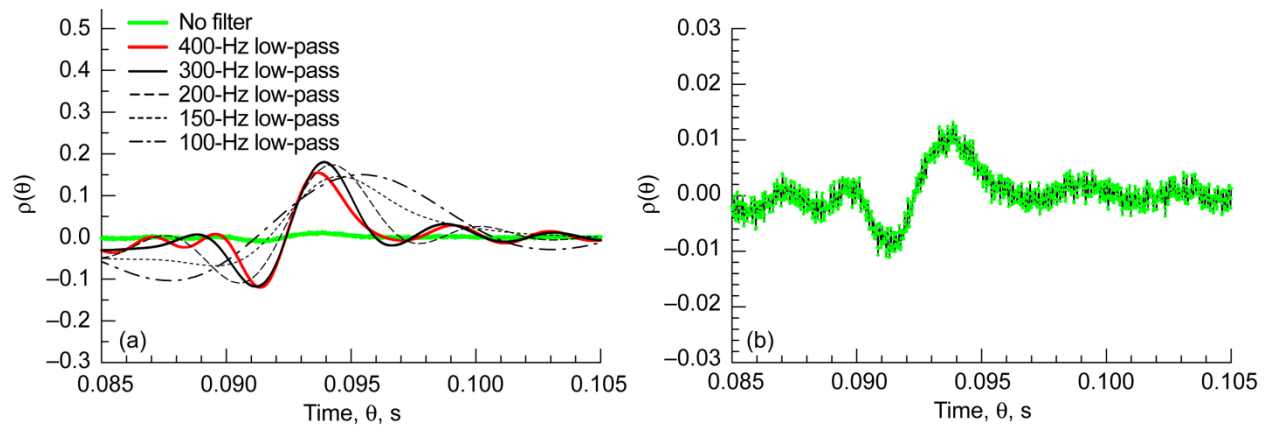


Figure 4.—Normalized cross-correlation, $\rho(\theta)$, using internal combustor pressure sensor and 110° far-field microphone, calculated using no filter and various low-pass filters at setting of 60 percent of maximum power in region of peak values. (a) 100- to 400-Hz low-pass filters. (b) No filter.

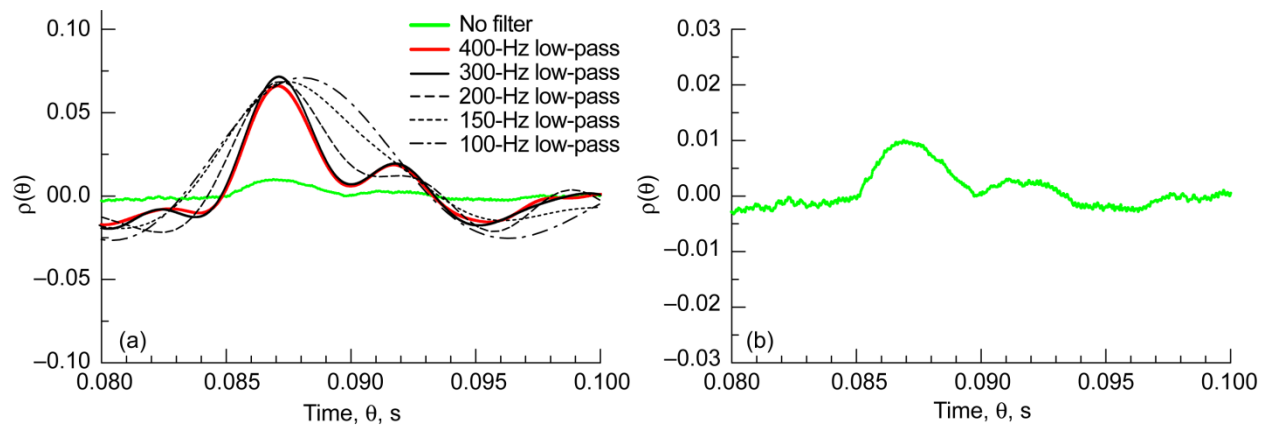


Figure 5.—Normalized cross-correlation, $\rho(\theta)$, using internal combustor pressure sensor and 110° far-field microphone, calculated using no filter and various low-pass filters at setting of 71 percent of maximum power in region of peak values. (a) 100- to 400-Hz low-pass filters. (b) No filter.

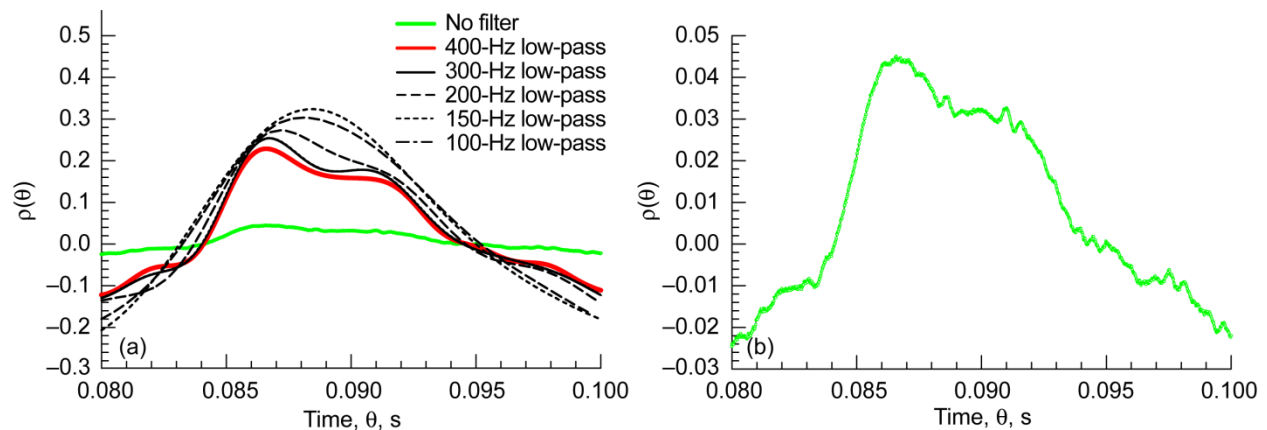


Figure 6.—Normalized cross-correlation, $\rho(\theta)$, using internal combustor pressure sensor and 160° far-field microphone, calculated using no filter and various low-pass filters at setting of 48 percent of maximum power in region of peak values. (a) 100- to 400-Hz low-pass filters. (b) No filter.

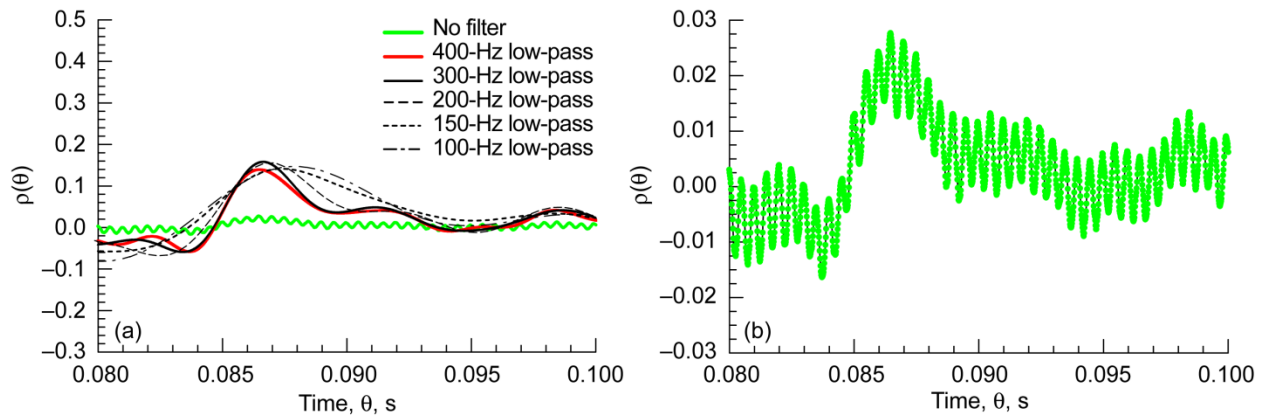


Figure 7.—Normalized cross-correlation, $\rho(\theta)$, using internal combustor pressure sensor and 160° far-field microphone, calculated using no filter and various low-pass filters at setting of 54 percent of maximum power in region of peak values. (a) 100- to 400-Hz low-pass filters. (b) No filter.

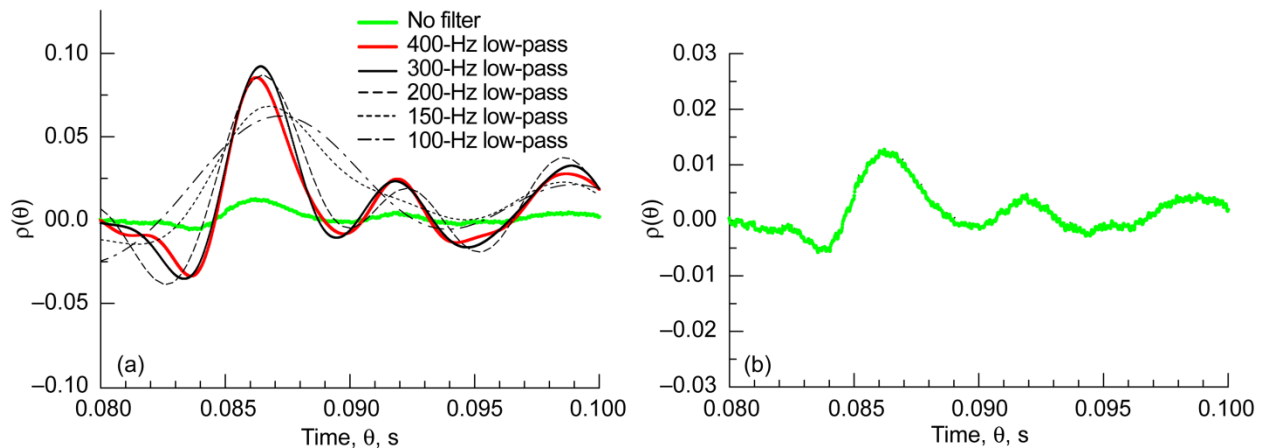


Figure 8.—Normalized cross-correlation, $\rho(\theta)$, using internal combustor pressure sensor and 160° far-field microphone, calculated using no filter and various low-pass filters at setting of 60 percent of maximum power in region of peak values. (a) 100- to 400-Hz low-pass filters. (b) No filter.

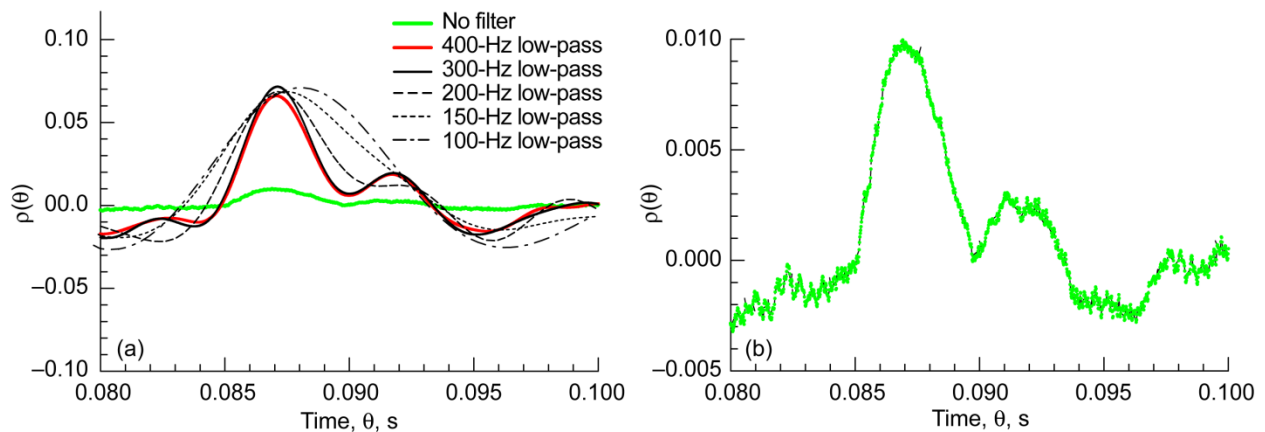


Figure 9.—Normalized cross-correlation, $\rho(\theta)$, using internal combustor pressure sensor and 160° far-field microphone, calculated using no filter and various low-pass filters at setting of 71 percent of maximum power in region of peak values. (a) 100- to 400-Hz low-pass filters. (b) No filter.

The cross-correlation of band-limited signals is smeared in the time domain. An example is shown in Figure 1 where various low-pass filters are used with white noise. Consequently, all the cross-correlation function show smeared peaks.

Figures 2 through 9 show that as the low-pass filter cutoff frequency η is decreased, more direct combustion noise, which controls the left side of the peak, is removed; the temporal smearing is increased; and the peak occurs at a longer time delay.

The normalized cross-correlation functions calculated using the 300- and 400-Hz low-pass filters shown in Figures 2 through 9 part (a) are line plots. The normalized cross-correlation function calculated using the 400-Hz low-pass filter is always beneath the one created using the 300-Hz low-pass filter. The normalized cross-correlation function calculated using no filter is the curve located near zero in these plots and is shown on a larger scale in the corresponding part (b) plots.

Unfiltered and low-pass-filtered cross-correlation functions between a combustor pressure sensor and a far-field microphone at 110° and 160° at the 54, 60, and 71 percent of maximum power settings showed a single time delay peak. However, at 48 percent of maximum power setting a single or double peak was observed depending on the low-pass filter cutoff frequency. The 48-percent operating condition cross-correlation functions showed a double peak when using signals unfiltered and filtered with cutoff frequencies of 300 and 400 Hz.

For the unfiltered cross-correlation and the cross-correlation filtered using a 400-Hz cutoff frequency at each power setting, the largest peak is at an acoustic time delay near 94 ms for the far-field microphone at 110°, near 90 ms for the far-field microphone at 130° (see Ref. 1), and near 86.5 ms for the far-field microphone at 160°. For the double-peak normalized cross-correlation function at the 48-percent operating condition the second peak is near 98 ms for the far-field microphone at 110° (Fig. 2), near 95 ms for the far-field microphone at 130° (see Ref. 1), and near 91 ms for the far-field microphone at 160° (Fig. 6). Consequently, the time delay using this process is 4 ms using the 110° far-field microphone (Fig. 2), 5 ms using the 130° far-field microphone, and 4.5 ms using the 160° far-field microphone (Fig. 6).

A double peak is shown in Figures 2 and 6 for the 48 percent of maximum power case. The highest peak in the cross-correlation of the unfiltered signals is due to the acoustic propagation time. The second peak may be due to the acoustic propagation time of the indirect combustion noise, or it may be due to some engine-related interference factor. To avoid subjective observations this study is based on using the filtering of the signals to change the ratio of acoustic signals due to direct combustion noise and acoustic signals due to indirect combustion noise. This is nonsubjective and facility independent. Filtering without introducing any phase shift does not change the propagation physics of the acoustic signals or entropy signals. The presence of the two peaks for the 48 percent of maximum power case cannot be avoided. However, they are not a feature present at all power settings. The filtering procedure can be applied at all power settings. Regardless, the location of the double- or single-peak maximum value shifts to larger time delays as the low-pass filter cutoff frequency is decreased, and this fact is an observable phenomenon.

At the three higher operating conditions the two-peak phenomenon is not observed in cross-correlations made using the combustor pressure sensor with the 110° and 160° far-field microphones. Only a single peak cross-correlation is observed. The reason only a single peak is detected is not clear, but it is possible that the relative amount of indirect combustion noise in the signal is decreased thus making its detection as a discrete peak more difficult at these three higher power settings. Another possibility is that the ripple that is observed at the 48 percent operating condition is due to a convective entropy feedback mechanism, which acts to enhance the indirect combustion noise signal for this case. However, in all cases the single peak or the left peak where a double peak occurs shifts to the right as the low-pass filter cutoff frequency is decreased.

The resulting delay time values of the peaks are shown in Table II for the far-field microphones at 110° and 160°. Peak values of the normalized cross-correlation function are shown in Table III for the far-field microphones at 110° and 160°.

TABLE II.—TIME DELAYS AT PEAK OF CROSS-CORRELATIONS
OF 110° AND 160° MICROPHONE SIGNALS AND
CIP1 COMBUSTOR PRESSURE SIGNAL

Percent engine power level, P	Time delay, τ , ms					
	Low-pass filter					
	None	400 Hz	300 Hz	200 Hz	≈ 150 Hz	100 Hz
(a) 110°						
48	94.06	93.83	94.06	94.65	95.29	95.70
54	93.63	93.90	94.16	94.71	95.12	95.76
60	93.86	93.67	93.92	94.24	94.54	95.43
71	94.16	94.24	94.38	94.56	94.77	95.57
(b) 160°						
48	86.58	86.59	86.72	87.17	88.09	88.42
54	86.46	86.47	86.64	86.91	87.39	87.89
60	86.21	86.24	86.43	86.49	86.76	87.19
71	86.90	87.07	87.11	87.16	87.46	88.06

TABLE III.—PEAK VALUES OF NORMALIZED CROSS-CORRELATION FUNCTIONS,
 $\rho(\theta)|_{\text{peak}}$, OF 110° AND 160° MICROPHONE SIGNALS AND
CIP1 COMBUSTOR PRESSURE SIGNAL

Percent engine power level, P	Low-pass filter					
	None	400 Hz	300 Hz	200 Hz	~ 150 Hz	100 Hz
(a) 110°						
48	0.020	0.210	0.249	0.299	0.341	0.383
54	0.015	0.181	0.212	0.217	0.201	0.214
60	0.013	0.155	0.181	0.174	0.146	0.150
71	0.010	0.128	0.152	0.141	0.115	0.110
(b) 160°						
48	0.045	0.229	0.254	0.273	0.303	0.324
54	0.028	0.139	0.158	0.156	0.141	0.147
60	0.013	0.086	0.092	0.087	0.068	0.062
71	0.010	0.066	0.072	0.069	0.069	0.071

Discussion

This section discusses the source separation relative time delays. The relative time delays are related to the direct and indirect combustion noise travel time. Then the enhancement of the normalized cross-correlation magnitude with filtering is presented.

Dependent Source Separation

An interpretation of the time delay for the peaks of the cross-correlation function shown in Table II for the 110° and 160° far-field microphones, respectively, and Table 7 of Reference 1 for the 130° far-field microphone can be made by plotting the relative time delay peaks of the cross-correlation functions, $\Delta\tau(\eta)|_{\text{peak}}$, where

$$\Delta\tau(\eta)|_{\text{peak}} = \tau(\eta)|_{\text{peak}} - \tau(\text{reference})|_{\text{peak}} \quad (4)$$

where $\Delta\tau(\eta)|_{\text{peak}}$ is the estimated indirect combustion noise time delay (identified as the estimated post-combustion, or post-flame, residence time of the entropy and combustion products in the cooled combustor section).

Two procedures are used herein to obtain a reference time delay. One procedure uses the time delay peak when the signals are analyzed with no filter. The second procedure uses the time delay peak when the signals are analyzed with the 400-Hz low-pass filter. In the next section, $\Delta\tau(\eta)|_{\text{peak}}$ is shown to be related to the post-combustion residence time of the entropy perturbations and combustion products, which travel in the cooled combustor section before they reach the turbine. The estimated indirect combustion noise time delay values (post-combustion residence time values) $\Delta\tau(\eta)|_{\text{peak}}$ are only approximate because the spectral distribution of direct and indirect combustion noise overlap.

These plots are shown two ways. In Figure 10, the variation of $\Delta\tau(\eta)|_{\text{peak}}$ as a function of η for each power setting is shown for each angle using the no-filter value as the reference. This produces figures where the maximum value is maximized and the traces for the 60 and 71 percent maximum power cases are similar. In Figure 11, the variation of $\Delta\tau(\eta)|_{\text{peak}}$ as a function of η for each power setting is shown for each angle using the 400-Hz low-pass filter value as the reference. While the maximum values are lower, the traces for each power setting are more separated.

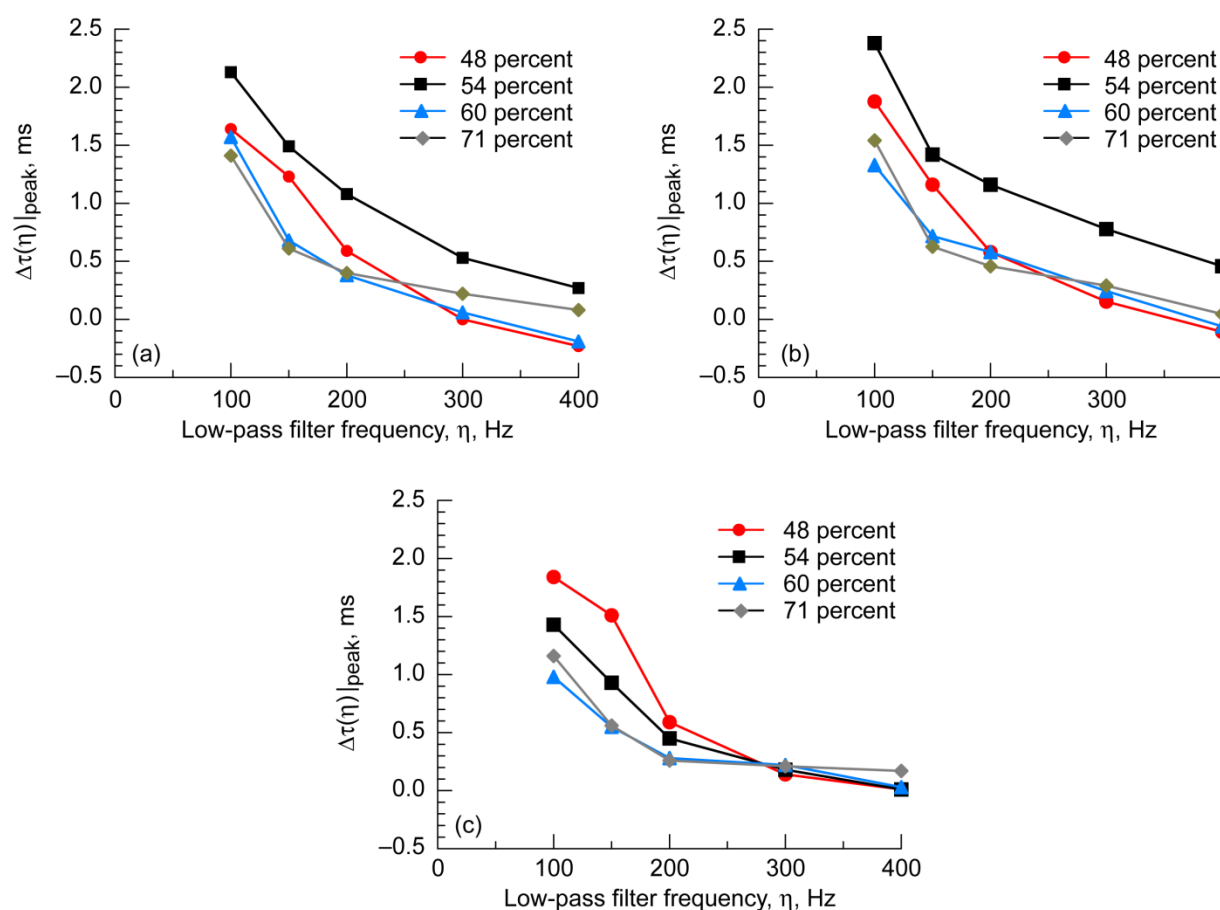


Figure 10.—For far-field microphones at 110°, 130°, and 160°, time delay at peak value of cross-correlation function $\Delta\tau(\eta)|_{\text{peak}}$ of low-pass-filtered signals relative to peak time delay using no filter as function of filter design frequency, η , for turbofan engine operating at 48, 54, 60, and 71 percent of maximum power. (a) 110°. (b) 130°. (c) 160°.

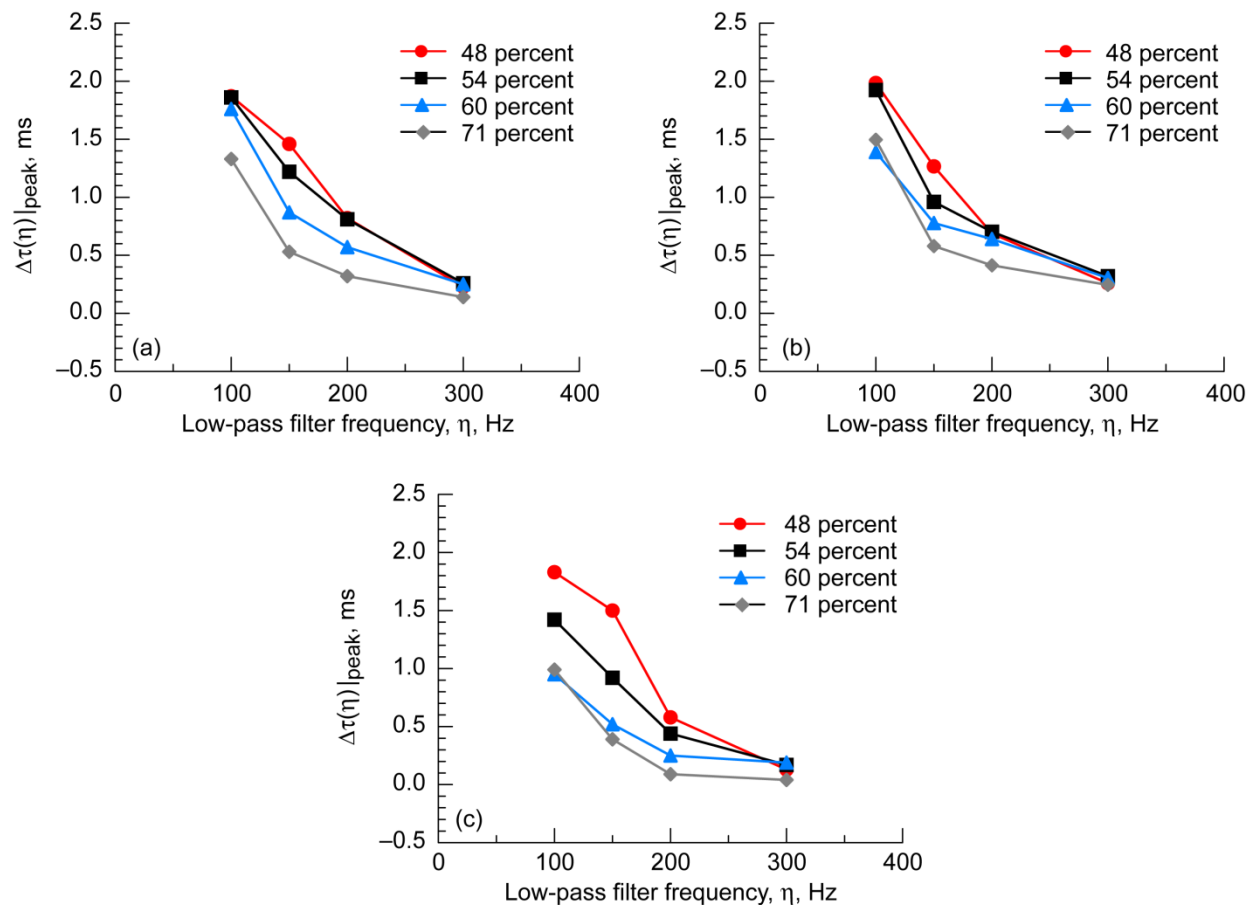


Figure 11.—For far-field microphones at 110°, 130°, and 160°, time delay at peak value of cross-correlation function $\Delta\tau(\eta)|_{\text{peak}}$ of low-pass-filtered signals relative to peak time delay using 400-Hz low-pass filter as function of filter design frequency, η , for turbfan engine operating at 48, 54, 60, and 71 percent of maximum power. (a) 110°. (b) 130°. (c) 160°.

In Figure 12, the values $\Delta\tau(\eta)|_{\text{peak}}$ as a function of η at each angle are shown for each power setting using the no-filter value as the reference. As the low-pass filter design cutoff frequency η is reduced, the time delays tend to increase because an decreasing amount of direct combustion noise is present. These results show low-pass filtering can be used to separate this type of dependent source.

In Figure 13, the values $\Delta\tau(\eta)|_{\text{peak}}$ as a function of η at each angle are shown for each power setting using the 400-Hz low-pass filter value as the reference. Again, as the low-pass filter design cutoff frequency η is reduced, the time delays tend to increase because an decreasing amount of direct combustion noise is present.

The results are more consistent when plotted for each turbfan engine operating setting as shown in Figure 12. The trace of the curves is less dependent on the microphone position and vary dependent on operating condition. The major discrepancy is at the 160° angular location for the 54 percent maximum power setting when the no filter reference is used. The grouping of the traces for each angle are a better match when the 400-Hz low-pass filter peak value is used as a reference. A significant noise source near 1400 Hz produces a significant ripple in the cross-correlation function for this case and makes it difficult to get a valid value for the peak. This ripple is clearly evident in Figures 7(a) and (b).

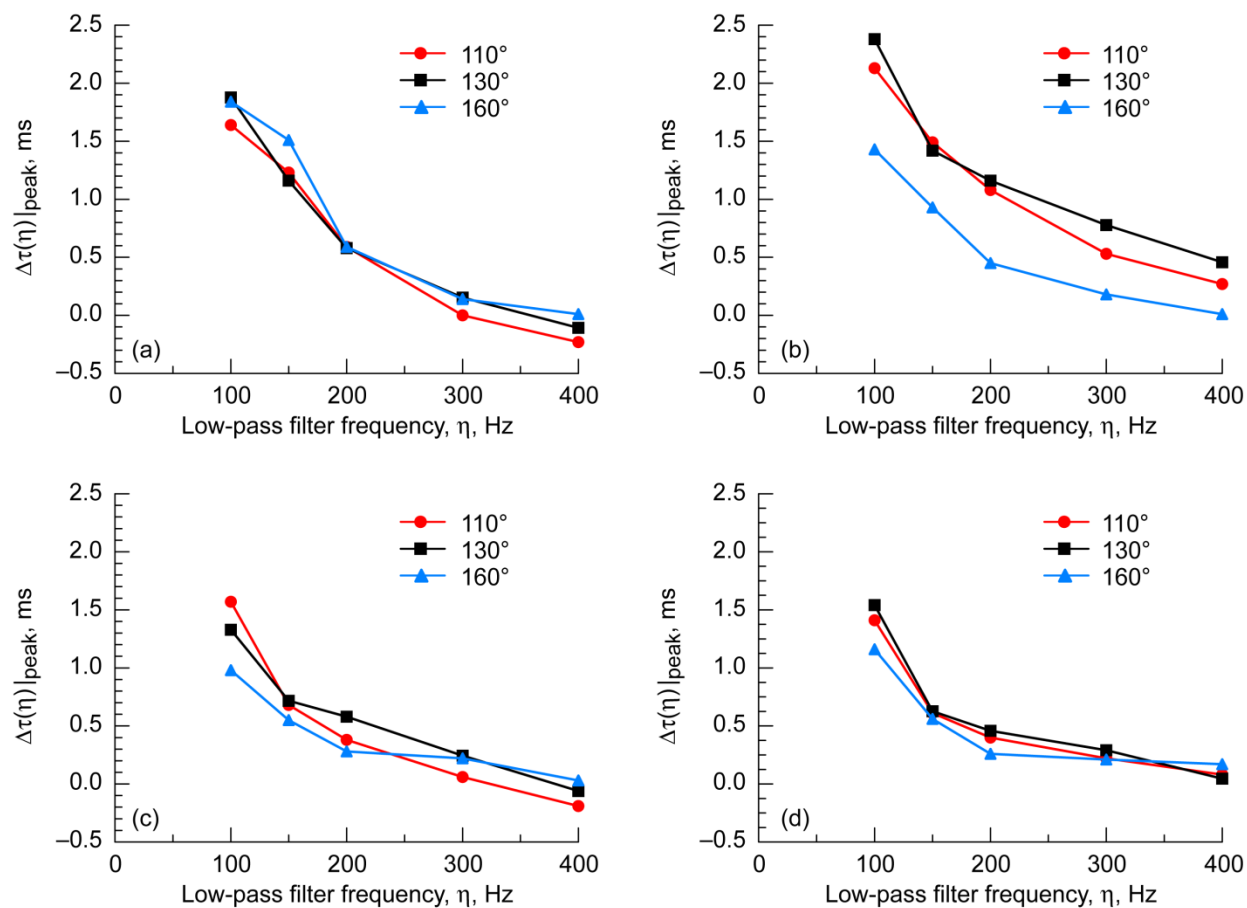


Figure 12.—For far-field microphones at 110°, 130°, and 160°, time delay at peak value of cross-correlation function $\Delta\tau(\eta)|_{\text{peak}}$ of low-pass-filtered signals relative to peak time delay using no filter as function of filter design frequency, η , for turbofan engine operating at 48, 54, 60, and 71 percent of maximum power. (a) 48 percent. (b) 54 percent. (c) 60 percent. (d) 71 percent.

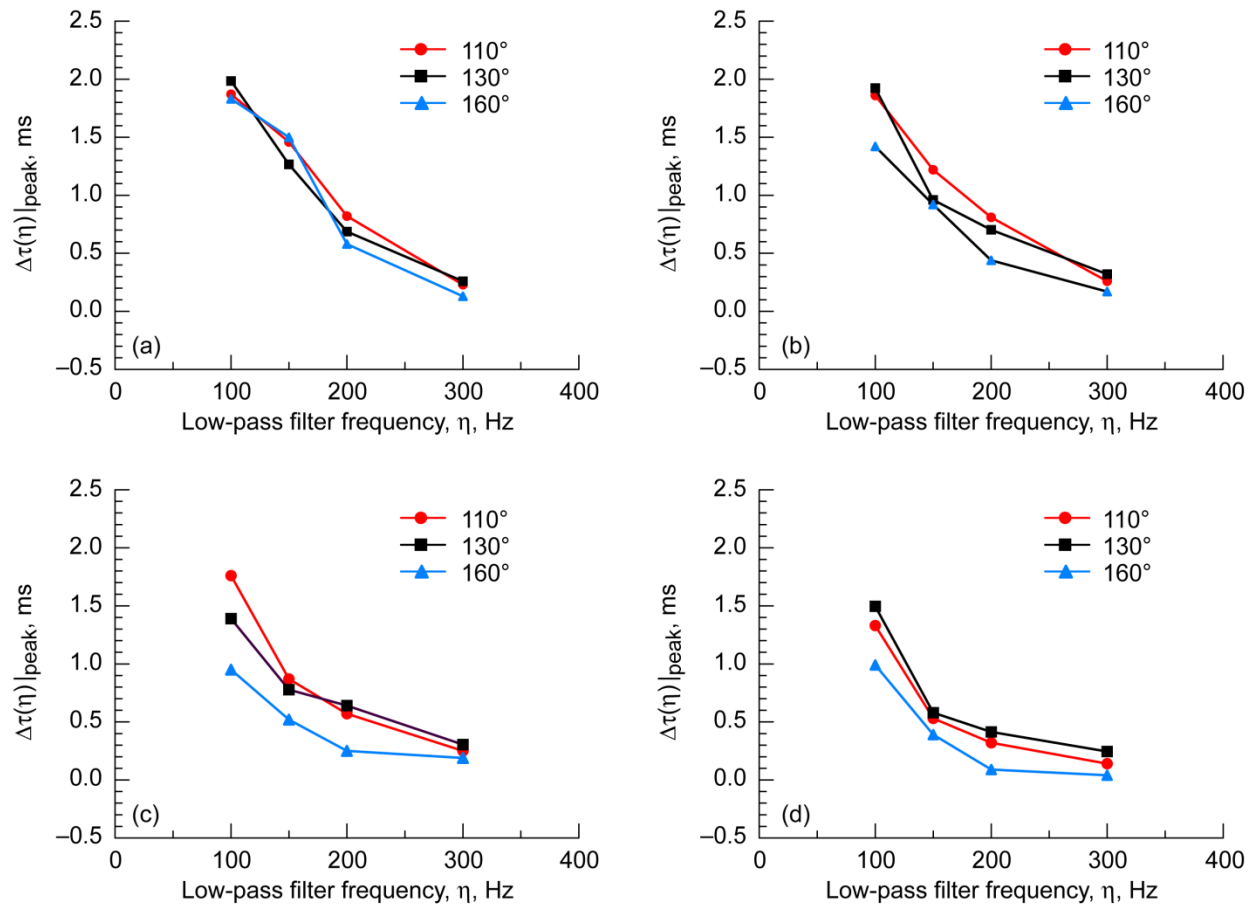


Figure 13.—For far-field microphones at 110°, 130°, and 160°, time delay at peak value of cross-correlation function $\Delta\tau(\eta)|_{\text{peak}}$ of low-pass-filtered signals relative to peak time delay using 400-Hz low-pass filter as function of filter design frequency, η , for turbofan engine operating at 48, 54, 60, and 71 percent of maximum power. (a) 48 percent. (b) 54 percent. (c) 60 percent. (d) 71 percent.

Propagation Time Evaluation Method

Evaluation of the propagation time using the cross-spectrum between a combustor pressure sensor and a far-field microphone at 30.5 m (100 ft) and 130° by Miles (Ref. 3) indicated the direct signal had a time delay of 86.98 ms and the indirect signal had a time delay of 90.03 ms. The difference is 3.05 ms, which is attributed to the entropy convecting with the flow before entering the turbine. The linear connection between entropy and pressure fluctuations found by Miles (Ref. 20) implies the direct and indirect combustion noise are dependent. The original concept was that the low-frequency core noise source was the combustor and the noise traveled upstream from the combustor through the nozzle. Let the distance the entropy disturbance travels to the turbine entrance be L_c and the radial distance from the engine to the far field microphone be r .

Fundamental to the interpretation of the results presented is that entropy waves (or hot spots) travel at the flow velocity v_s , which is only a fraction of the speed of sound. According to Hill and Peterson (Ref. 21), the average axial velocity of the combustor reactants v_s is on the order of 30 m/s (98 ft/s).

The speed of sound in a combustor c_c is generally calculated based on the assumption that the air is a perfect gas (Refs. 22 and 23):

$$c_c = \sqrt{\frac{\gamma \Re \mathfrak{T}_c}{W}} \quad (5)$$

where γ is the specific heat ratio, or adiabatic index, 1.4; \Re is the molar gas constant, 8.3145 J/mol·K; and W is the molar mass of air, 0.029 kg/mol.

As reported by Hill and Peterson (Ref. 21), typical turbine inlet temperatures \mathfrak{T}_c are on the order of 1600 K (2880 °R). Consequently, the speed of sound c_c is on the order of 800 m/s.

Thus the direct combustion noise time of travel τ_d is

$$\tau_d = 87.2 \text{ ms} = \frac{L_c}{v_s + c_c} + \frac{\tau}{c_o} \quad (6)$$

where $L_c = 0.095$ m, $v_s = 30$ m/s, $c_c = 800$ m/s, $\tau = 30.48$ m, the speed of sound in air $c_o = 350$ m/s, and the acoustic travel time in the tailpipe is neglected since it is small and the same for all the sources.

The indirect combustion noise time of travel τ_i is

$$\tau_i = 90.11 \text{ ms} = \frac{L_c}{v_s} + \frac{\tau}{c_o} \quad (7)$$

Consequently, the indirect combustion noise time delay (post-combustion, or post-flame, residence time) of the entropy and combustion products in the cooled combustor section $\Delta\tau$ can be approximated by subtracting the acoustic travel time of the direct combustion noise to the far-field microphone τ_d from the travel time of the indirect combustion noise to the far-field microphone τ_i :

$$\Delta\tau = \tau_i - \tau_d = 3.052 \text{ ms} = L_c \left(\frac{1}{v_s} - \frac{1}{(v_s + c_c)} \right) \approx \frac{L_c}{v_s} \quad (8)$$

This theoretical post-combustion residence time, $\Delta\tau$, is to be compared to the estimated post-combustion residence time values $\Delta\tau(\eta)|_{\text{peak}}$ shown in Figures 10 to 13, which were calculated using Equation (4).

As dependent time histories, these two sources are separated by the cross-spectrum procedure. However, the separation is not as clearly displayed using the cross-correlation method, where the separation does increase as the filter frequency η is reduced, but reaches a maximum value near 2.5 ms. This time delay measurement discrepancy is attributed to difficulties in sufficiently separating the mixture of indirect combustion noise in the 0 to 200 Hz frequency range from the direct combustion noise in the 200 to 400 Hz frequency range. This problem also appears in results obtained by Miles in Reference 1 using the 150-Hz low-pass filtered signals with the cross-spectrum method; it can be seen in Figures 15 and 16 of that paper that the use of a time delay of 86.98 ms creates a flat phase angle between 200 and 300 Hz, shown in Figure 16(c), indicating this is the direct combustion noise location (fast propagation speed), whereas using a time delay of 90.03 ms creates flat phase angle between 0 and 200 Hz, shown in Figure 15(c), indicating this is the indirect combustion noise location (slow propagation speed). Using this 150-Hz low-pass filter still leaves the signals so intermixed that one is barely able to distinguish between direct and indirect combustion noise. In addition, as the low-pass filter frequency is reduced the cross-correlation peaks in the time domain get wider.

Identifying the sources creating a system output signal is generally achieved using specific tagged input test signals. For the turbofan engine combustion noise problem this is difficult, and we must depend currently on tagged signals created by the system. Consequently, using the cross-correlation procedure or the low-pass filtering procedure we arrive at viewing the output signal as being a blend of indirect

combustion noise, which is loudest in the 0 to 200 Hz frequency range and has a longer propagation time to the far field, and direct combustion noise, which is loudest in the 200 to 400 Hz frequency range and has a quicker propagation time to the far field. However, the indirect and direct combustion noise source frequency ranges overlap for this engine, and as a consequence low-pass filtering as implemented herein is not as useful as one would hope in separating the direct and indirect combustion noise. One needs a way to study the blending as a function of frequency. However, these results do show that low-pass filtering can be used with the cross-correlation function to separate this type of dependent source to some extent and confirm the cross-spectrum results. The fact that both methods do create separation to some extent give credence to the hypothesis that the far-field low-frequency core noise is due to a blend of direct and indirect combustion noise for this engine. Detailed information on how the signals are blended or mixed as a function of frequency is not available and must be the subject of further investigation. In addition, it might be a function of engine design as well as operating condition. Determining the mixture or blend as a function of frequency of direct and indirect combustion noise is an important research objective. However, the first step is to show that an indirect combustion noise source is responsible for part of the far-field turbofan engine noise spectrum.

Identification of Combustion Noise

As previously shown by Miles (Ref. 1) using the 130° far-field microphone, Table III shows that filtering can increase the correlation function significantly. A low-pass filter in the range of 200 to 300 Hz works well for this particular turbofan engine.

Concluding Remarks

Low-pass filtering with a 100-Hz cutoff frequency to remove a large amount of the direct combustion noise leaves the indirect combustion noise, which has approximately a relative time delay of 1 to 2.5 ms. This time delay is longer than the time delay observed with no filtering or low-pass filtering at 400 Hz. This shows that some of the direct combustion noise, which is always traveling at the speed of sound, has been removed leaving the indirect combustion noise, which spends some time moving convectively at a much lower velocity than the speed of sound in the combustor. As a consequence of removing part of the combustion noise that travels fastest, the delay time of the combustion noise remaining in the signal is greater. The largest indirect combustion noise time delay found using this procedure is about 2 ms. The cross-correlation function, when used with low-pass filtering, is very useful in separating the indirect and direct combustion noise source in this system.

Coherence analysis using the cross-spectrum phase angle method separates direct and indirect combustion noise using filtered or unfiltered signals. This is done by an examination of the effect that use of different time delays has on the phase angle of the cross-spectrum calculated using the combustor pressure sensor signal and a far-field microphone signal. For the cross-spectrum between a combustor pressure sensor and a far-field microphone at 130°, this method indicated the direct signal had a time delay of 86.98 ms and the indirect signal had a time delay of 90.03 ms. The indirect combustion noise time delay time is thus 3.05 ms.

This time delay measurement discrepancy is attributed to difficulties in sufficiently separating the mixture of indirect combustion noise in the 0 to 200 Hz frequency range from the direct combustion noise in the 200 to 400 Hz frequency range. In addition, as the low-pass filter frequency is reduced the cross-correlation peaks in the time domain get wider. These results do show that low-pass filtering can be used with the cross-correlation function to separate this type of dependent source to some extent and confirm the cross-spectrum results.

For the 48 percent of maximum power case two peaks separated by 4 to 4.5 ms were measured. If these peaks are due to direct and indirect combustion noise this would show that some of the direct combustion noise, which is always traveling at the speed of sound, is responsible for the peak at the shortest time and that the indirect combustion noise, which spends some time moving convectively

at a much lower velocity than the speed of sound in the combustor, is responsible for the peak at the longer time.

Examination of the results using the three different far-field microphones shows that the post-combustion times measured at each angle are fairly consistent with one another at a given operating condition. The results may lead to a better idea about the acoustics in the combustor and may help develop and validate improved reduced-order physics-based methods for predicting direct and indirect combustion noise.

Appendix—Symbols

B_e	effective spectral resolution bandwidth
c	speed of sound
D	propagation time delay for sound to travel from engine to microphone
f	frequency
L	length
N	segment length, (data points)/segment
n	number
P	percent of maximum power
R	correlation function
\mathfrak{R}	molar gas constant, 8.3145 J/mol·K
r	rate
τ	radial distance from engine to far-field microphone
T	time interval
\mathcal{T}	record length
\mathfrak{T}	temperature
t	time
v	flow speed
W	molar mass of air, 0.029 kg/mol
x, y	signal time histories
γ	specific heat ratio, or adiabatic index, 1.4
η	cutoff frequency of low-pass filter
θ	time shift
ρ	normalized cross-correlation function, normalized cross-correlation function coefficient, or normalized cross-covariance function
τ	signal travel time
$\Delta\tau$	analytical combustion noise time delay; also the post-combustion (post-flame) residence time
$\Delta\tau(\eta) _{\text{peak}}$	estimated indirect combustion noise time delay; also the estimated post-combustion (post-flame) residence time
ϕ	angle of microphone relative to engine

Subscripts:

c	combustor
d	direct
e	effective
f	frequency
i	indirect
n	number
o	in air

<i>s</i>	entropy
<i>ss</i>	sample segment
<i>tot</i>	total
<i>u</i>	upper
<i>x, y</i>	signal time histories

References

1. Miles, Jeffrey: Core Noise Diagnostics of Turbofan Engine Noise Using Correlation and Coherence Functions. *J. Propul. Power* (NASA/TM—2009-215609 and AIAA-2009-1237), vol. 26, no. 2, 2010, pp. 303–316.
2. Miles, J.H.: Separating Direct and Indirect Turbofan Engine Combustion Noise Using the Correlation Function. *J. Propul. Power*, vol. 26, no. 5, 2010, pp. 1144–1152.
3. Miles, Jeffrey Hilton: Spectral Separation of the Turbofan Engine Coherent Combustion Noise Component. NASA/TM—2008-215157 (AIAA-2008-50), 2008.
4. Miles, Jeffrey Hilton: Time Delay Analysis of Turbofan Engine Direct and Indirect Combustion Noise Sources. *J. Propul. Power*, vol. 25, no. 1, 2009, pp. 218–227.
5. Mendoza, Jeff; Nance, Don; and Ahuja, K.: Source Separation From Multiple Microphone Measurements in the Far Field of a Full Scale Aero Engine. AIAA-2008-2809, 2008.
6. Weir, Donald; and Mendoza, Jeffrey: Baseline Noise Measurements From the Engine Validation of Noise and Emissions Reduction Technology Program. AIAA-2008-2807, 2008.
7. Schuster, Bill: Statistical Considerations for Gas Turbine Engine Noise Measurements. AIAA-2008-2808, 2008.
8. Royalty, Charles; and Schuster, Bill: Noise From a Turbofan Engine Without a Fan From the Engine Validation of Noise and Emission Reduction Technology (EVNERT) Program. AIAA-2008-2810, 2008.
9. Dougherty, Robert P.; and Mendoza, Jeff: Nacelle In-Duct Beamforming Using Modal Steering Vectors. AIAA-2008-2812, 2008.
10. Weir, Don, ed.: Engine Validation of Noise and Emission Reduction Technology Phase I. NASA/CR— 2008-215225 (Honeywell Report No. 21-13843A), 2008.
11. Hultgren, Lennart; and Miles, Jeffrey: Noise-Source Separation Using Internal and Far-Field Sensors for a Full-Scale Turbofan Engine. AIAA-2009-3220, 2009.
12. Carter, G. Clifford, ed.: Tutorial Overview of Coherence and Time Delay Estimation. *Coherence and Time Delay Estimation: An Applied Tutorial for Research, Development, Test, and Evaluation Engineers*, Pt. 1, IEEE Press, Piscataway, NJ, 1993, pp. 1–27.
13. Scarbrough, K.; Ahmed, N.; and Carter, G.: On the Simulation of a Class of Time Delay Estimation Algorithms. *IEEE Trans. Acoust. Speech Signal Process.*, vol. ASSP-29, no. 3, 1981, pp. 534–540.
14. Bendat, Julius S.; and Piersol, Allan G.: *Random Data; Analysis and Measurement Procedures*. Wiley-Interscience, New York, NY, 1971.
15. Bendat, Julius S.; and Piersol, Allan G.: *Engineering Applications of Correlation and Spectral Analysis*. Wiley-Interscience, New York, NY, 1980.
16. Stearns, Samuel D.; and David, Ruth A.: *Signal Processing Algorithms Using Fortran and C*. Prentice-Hall, Englewood Cliffs, NJ, 1993.
17. Kormylo, J.; and Jain, V.: Two-Pass Recursive Digital Filter With Zero Phase Shift. *IEEE Trans. Acoust. Speech Signal Process.*, vol. 22, no. 5, 1974, pp. 384–387.
18. Hamming, R.W.: *Digital Filters*. Third ed., Dover Publications, Mineola, NY, 1998.
19. Matsumoto, Makoto; and Nishimura, Takuji: Mersenne Twister: A 623-Dimensionally Equidistributed Uniform Pseudo-Random Number Generator. *ACM Trans. Model. Comput. Simul.*, vol. 8, no. 1, 1998, pp. 3–30.
20. Miles, J.H.; Wasserbauer, C.A.; and Krejsa, E.: Cross Spectra Between Temperature and Pressure in a Constant Area Duct Downstream of a Combustor. AIAA-83-0762 (NASA TM-83351), 1983.
21. Hill, Philip G.; and Peterson, Carl R.: *Mechanics and Thermodynamics of Propulsion*. Second ed., Addison-Wesley, Reading, MA, 1992.
22. Poinot, Thierry; and Veynante, Denis: *Theoretical and Numerical Combustion*. Second ed., Edwards, Philadelphia, PA, 2005.
23. Lieuwen, Timothy C.; and Yang, Vigor: *Combustion Instabilities in Gas Turbine Engines: Operational Experience, Fundamental Mechanisms and Modeling*. AIAA, Reston, VA, 2005.

REPORT DOCUMENTATION PAGE			Form Approved OMB No. 0704-0188		
<p>The public reporting burden for this collection of information is estimated to average 1 hour per response, including the time for reviewing instructions, searching existing data sources, gathering and maintaining the data needed, and completing and reviewing the collection of information. Send comments regarding this burden estimate or any other aspect of this collection of information, including suggestions for reducing this burden, to Department of Defense, Washington Headquarters Services, Directorate for Information Operations and Reports (0704-0188), 1215 Jefferson Davis Highway, Suite 1204, Arlington, VA 22202-4302. Respondents should be aware that notwithstanding any other provision of law, no person shall be subject to any penalty for failing to comply with a collection of information if it does not display a currently valid OMB control number.</p> <p>PLEASE DO NOT RETURN YOUR FORM TO THE ABOVE ADDRESS.</p>					
1. REPORT DATE (DD-MM-YYYY) 01-05-2011		2. REPORT TYPE Technical Memorandum		3. DATES COVERED (From - To)	
4. TITLE AND SUBTITLE Separating Direct and Indirect Turbofan Engine Combustion Noise While Estimating Post-Combustion (Post-Flame) Residence Time Using the Correlation Function		5a. CONTRACT NUMBER			
		5b. GRANT NUMBER			
		5c. PROGRAM ELEMENT NUMBER			
6. AUTHOR(S) Miles, Jeffrey, Hilton		5d. PROJECT NUMBER			
		5e. TASK NUMBER			
		5f. WORK UNIT NUMBER WBS 561581.02.08.03.18.03			
7. PERFORMING ORGANIZATION NAME(S) AND ADDRESS(ES) National Aeronautics and Space Administration John H. Glenn Research Center at Lewis Field Cleveland, Ohio 44135-3191		8. PERFORMING ORGANIZATION REPORT NUMBER E-17235			
9. SPONSORING/MONITORING AGENCY NAME(S) AND ADDRESS(ES) National Aeronautics and Space Administration Washington, DC 20546-0001		10. SPONSORING/MONITOR'S ACRONYM(S) NASA			
		11. SPONSORING/MONITORING REPORT NUMBER NASA/TM-2011-216248			
12. DISTRIBUTION/AVAILABILITY STATEMENT Unclassified-Unlimited Subject Category: 71 Available electronically at http://www.sti.nasa.gov This publication is available from the NASA Center for AeroSpace Information, 443-757-5802					
13. SUPPLEMENTARY NOTES					
14. ABSTRACT A previous investigation on the presence of direct and indirect combustion noise for a full-scale turbofan engine using a far-field microphone at 130° is extended by also examining signals obtained at two additional downstream directions using far-field microphones at 110° and 160°. A generalized cross-correlation function technique is used to study the change in propagation time to the far field of the combined direct and indirect combustion noise signal as a sequence of low-pass filters are applied. The filtering procedure used produces no phase distortion. As the low-pass filter frequency is decreased, the travel time increases because the relative amount of direct combustion noise is reduced. The indirect combustion noise signal travels more slowly because in the combustor entropy fluctuations move with the flow velocity, which is slow compared to the local speed of sound. The indirect combustion noise signal travels at acoustic velocities after reaching the turbine and being converted into an acoustic signal. The direct combustion noise is always propagating at acoustic velocities. The results show that the estimated indirect combustion noise time delay values (post-combustion residence times) measured at each angle are fairly consistent with one another for a relevant range of operating conditions and demonstrate source separation of a mixture of direct and indirect combustion noise. The results may lead to a better idea about the acoustics in the combustor and may help develop and validate improved reduced-order physics-based methods for predicting turbofan engine core noise.					
15. SUBJECT TERMS Combustion noise; Core noise; Correlation function; Coherence function					
16. SECURITY CLASSIFICATION OF:			17. LIMITATION OF ABSTRACT UU	18. NUMBER OF PAGES 27	19a. NAME OF RESPONSIBLE PERSON STI Help Desk (email: help@sti.nasa.gov)
a. REPORT U	b. ABSTRACT U	c. THIS PAGE U			19b. TELEPHONE NUMBER (include area code) 443-757-5802

